








OPEN

Biotic soil-plant interaction processes explain most of hysteric soil CO₂ efflux response to temperature in cross-factorial mesocosm experiment

Yann Dusza ^{1*}, Enrique P. Sanchez-Cañete ², Jean-François Le Galliard ^{1,3}, Régis Ferrière ^{4,5}, Simon Chollet ¹, Florent Massol ¹, Amandine Hansart¹, Sabrina Juarez¹, Katerina Dontsova ⁶, Joost van Haren⁶, Peter Troch^{6,7}, Mitchell A. Pavao-Zuckerman⁸, Erik Hamerlynck⁹ & Greg A. Barron-Gafford ^{6,10}

Ecosystem carbon flux partitioning is strongly influenced by poorly constrained soil CO₂ efflux (F_{soil}). Simple model applications (Arrhenius and Q_{10}) do not account for observed diel hysteresis between F_{soil} and soil temperature. How this hysteresis emerges and how it will respond to variation in vegetation or soil moisture remains unknown. We used an ecosystem-level experimental system to independently control potential abiotic and biotic drivers of the F_{soil} -T hysteresis. We hypothesized a principally biological cause for the hysteresis. Alternatively, F_{soil} hysteresis is primarily driven by thermal convection through the soil profile. We conducted experiments under normal, fluctuating diurnal soil temperatures and under conditions where we held soil temperature near constant. We found (i) significant and nearly equal amplitudes of hysteresis regardless of soil temperature regime, and (ii) the amplitude of hysteresis was most closely tied to baseline rates of F_{soil} , which were mostly driven by photosynthetic rates. Together, these findings suggest a more biologically-driven mechanism associated with photosynthate transport in yielding the observed patterns of soil CO₂ efflux being out of sync with soil temperature. These findings should be considered on future partitioning models of ecosystem respiration.

A major challenge in terrestrial carbon science is identifying atmospheric CO₂ source and sink dynamics across numerous timescales¹⁻³. Because CO₂ efflux (F_{soil}) can be the largest and most variable component flux in many ecosystems⁴, F_{soil} drives regional carbon dynamics^{5,6}. Accurate measurements of F_{soil} are critical for partitioning net ecosystem CO₂ flux (NEE) and modeling local-to-global carbon dynamics^{4,7,8}. Nighttime ecosystem respiration (R_{eco}) can be un-measurable using the eddy covariance (EC) technique because of a lack of turbulence and atmospheric mixing, requiring gap-filling procedures to produce credible sums⁷. These missing nighttime

¹Centre de recherche en écologie expérimentale et prédictive (CEREEP-Ecotron IleDeFrance), Département de biologie, Ecole normale supérieure, CNRS, PSL University, 77140, St-Pierre-les-Nemours, France. ²Departamento de Física Aplicada, Universidad de Granada, 18071, Granada, Spain. ³Sorbonne Université, CNRS, Institut d'Écologie et des Sciences de l'Environnement de Paris (iEES-Paris), Faculté des Sciences et Ingénierie, 75005, Paris, France. ⁴Institut de Biologie de l'Ens (IBENS), Département de biologie, Ecole normale supérieure, CNRS, PSL University, 75005, Paris, France. ⁵Department of Ecology and Evolutionary Biology, University of Arizona, Tucson, Arizona, 85721, United States. ⁶Biosphere 2, Office of Research, Development, & Innovation, University of Arizona, Tucson, Arizona, 85721, United States. ⁷Department of Hydrology & Atmospheric Sciences, University of Arizona, Tucson, Arizona, 85721, United States. ⁸Department of Environmental Science and Technology, University of Maryland, College Park, Maryland, 20742, United States. ⁹US Department of Agriculture-Agricultural Research Service, Eastern Oregon Agricultural Research Center, Burns, OR, 97720, United States. ¹⁰School of Geography & Development, University of Arizona, Tucson, Arizona, 85721, United States. *email: y.dusza@gmail.com

and all-daytime estimates of R_{eco} are often approximated using an exponential temperature (T)- R_{eco} regression model derived from nighttime EC data and T , which assumes that the diel temperature sensitivity can be fit using an Arrhenius or Q_{10} model^{8–10}. Incorrect daytime R_{eco} confounds NEE partitioning into R_{eco} and gross ecosystem productivity (GEP). Therefore, an incorrect model to estimate R_{eco} leads to greater uncertainty and bias in local-to-global estimates of NEE and its components. Some have suggested that the primary factors limiting our ability to characterize soil carbon metabolism and CO_2 efflux include lags and antecedent features of abiotic and biotic drivers associated with above- and belowground processes^{10–14}.

Considerable progress has been made in F_{soil} modeling by moving beyond simple temperature response functions (see¹⁵) to developing frameworks that account for multiple vegetative cover types or soil microhabitats^{16–19} and incorporate the important, but variable, influence of antecedent environmental effects^{20,21} and biotic inputs¹⁴. Still, our limited understanding of abiotic (e.g., environmental) and biotic (e.g., aboveground plant function) interactions constrains robust modeling of F_{soil} ^{12,22–24}. Many studies have shown that Arrhenius¹⁵ or Q_{10} ²⁵ functions poorly describe temperature dependence of F_{soil} – globally, and regardless of ecosystem type. Instead, F_{soil} often demonstrates a hysteretic response with temperature^{11,26–42}. In a hysteretic relationship, the dependent variable can be at multiple states for a given value of the explanatory variable depending on the system's history. Here, this means that a model based on a T (the explanatory variable) can give you two different estimates of F_{soil} (the dependent variable). How, then, can we expect numerical modeling to capture and appropriately predict rates of this dominant carbon source to the atmosphere, when we know the primary numerical relationship is so flawed? Both biological and physical processes can cause this hysteresis. Biological processes driving F_{soil} hysteresis might include patterns of photosynthate allocation^{12,14,33}, physiological upregulation⁴³, phenology^{13,14}, soil water redistribution^{21,44,45}, and dynamic storage and loss of carbon in response to micrometeorology^{27,36,46–50}.

Physical processes contributing to observed decoupling of F_{soil} from T include heat transport and gas diffusion through the soil⁵¹. For example, hysteresis can increase with soil drying because of decreased thermal diffusivity^{29,33}, or increase with soil wetting because of decreased gas diffusivity⁵². While a lack of observed T - F_{soil} relationships under field conditions does not negate theories of biological or enzymatic temperature dependence²³, hysteresis complicates prediction of surface CO_2 efflux and requires improved model formulations. Previous efforts to distinguish these physical processes from the influence of biological substrate inputs have been hindered, in part, by the lack of an ability to control meso-scale temperature of a soil column that could differentially regulate these contributing drivers.

The central question we address here is: what is the relative contribution of biotic and abiotic drivers in determining the hysteretic relationship between F_{soil} and temperature and how do these contributions vary across environmental gradients of moisture? We explore this question under semiarid conditions with semiarid vegetation. Semiarid regions experience multiple wet-dry transitions that create simultaneous ‘pulses’ of biological activity and alterations to the physical characteristics of the ecosystem⁴⁵ – making them an ideal setting for attempting to detangle these biotic and abiotic drivers. We hypothesized that lag in the delivery of recent photosynthate to soil leads to a hysteretic relationship between F_{soil} and temperature and that this lag increases with increased input from the plant (associated with the leaf area and net photosynthetic rates). In fact, previous studies have found this hysteretic relationship to be more prominent under woody plants than under grasses or bare soils³³. As such, wetter conditions, which are likely to stimulate photosynthate production and transport, might induce greater hysteresis in the relationship between F_{soil} and temperature. The alternate hypothesis is that hysteresis follows the decoupling of soil T relative to F_{soil} , not stimulation of F_{soil} by photosynthate. As noted by Phillips *et al.*⁵¹, the hysteretic response is likely due to the influence of both of these factors.

How biotic and abiotic drivers modulate patterns of F_{soil} in the context of mixed vegetation ecosystems is difficult to assess because of the potential, and variable, role they may play in driving fluxes. Therefore, the objectives of this study were to (i) quantify the response of F_{soil} to temperature, soil water content, and leaf-level carbon gain in a suite of controlled mesocosms and (ii) determine the relative influence of abiotic (soil temperature and soil water content) and biotic (photosynthesis) factors on F_{soil} rates and the amplitude of any hysteretic response to soil T across a range of moisture conditions. Within each mesocosm, we monitored air temperature, soil temperature, soil moisture, and soil CO_2 concentration continuously for two-week periods. At the same time, we measured rates of net photosynthesis of the vegetation to assess aboveground patterns of productivity. Then, we integrated these datasets. Because we wanted to understand the role of vegetative structure in determining the hysteretic relationship between T and F_{soil} , we repeated these suites of measurements across mesocosms that contained (i) bare soil, (ii) bunchgrass, (iii) woody plants, or (iv) a mixture of both bunchgrass and woody plants.

Results

Environmental control and mesocosm vegetative development. Tight regulation of soil temperature allowed us to create contrasting treatments in terms of a fluctuating diel pattern in soil temperature (30.88 ± 8.17 °C, representative of natural patterns; Fig. 1a) versus one with near-constant, modulated conditions (29.80 ± 2.43 °C; Fig. 1b). Similarly, precise irrigation yielded significant differences in treatment conditions between well-watered and dry soil moisture states (at 5 cm, 19.91 ± 0.57 versus $6.89 \pm 0.37\%$, respectively).

The two vegetation types utilized here are the grass *Bouteloua curtipendula* and the woody plant velvet mesquite (*Prosopis velutina* Woot.), representing fundamentally different growth forms. The grass is shallow-rooted, but produces a dense network of roots that occupy the upper ~30 cm of soil. The woody mesquite utilizes a network of shallow and deeper roots. As such, the grass has a significantly greater mass of fine and coarse roots driving near-surface soil CO_2 efflux than does mesquite ($p < 0.001$; grass and mesquite root biomass averaged 24.15 ± 6.49 and 2.65 ± 1.30 g, respectively; see Supplementary Table 1).

Relationship between diel soil CO_2 efflux and soil temperature, soil moisture, and aboveground plant function. Throughout the experiment, we observed the same elliptical shape and clockwise direction in the hysteretic relationship between soil temperature and F_{soil} for each vegetation type, regardless of the imposed

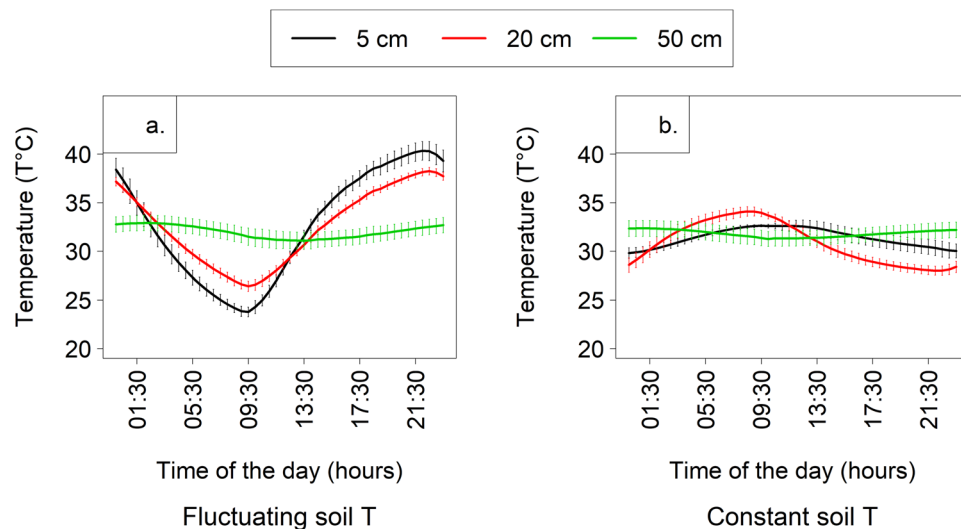


Figure 1. Average diel soil temperatures 5, 20, and 50 cm depths within Ecolabs set to mimic (a) typical, fluctuating diurnal pattern and (b) relatively constant soil temperatures. Atmospheric CO₂ concentrations and diel patterns of air temperature and the timing and intensity of light remained similar between these two treatments.

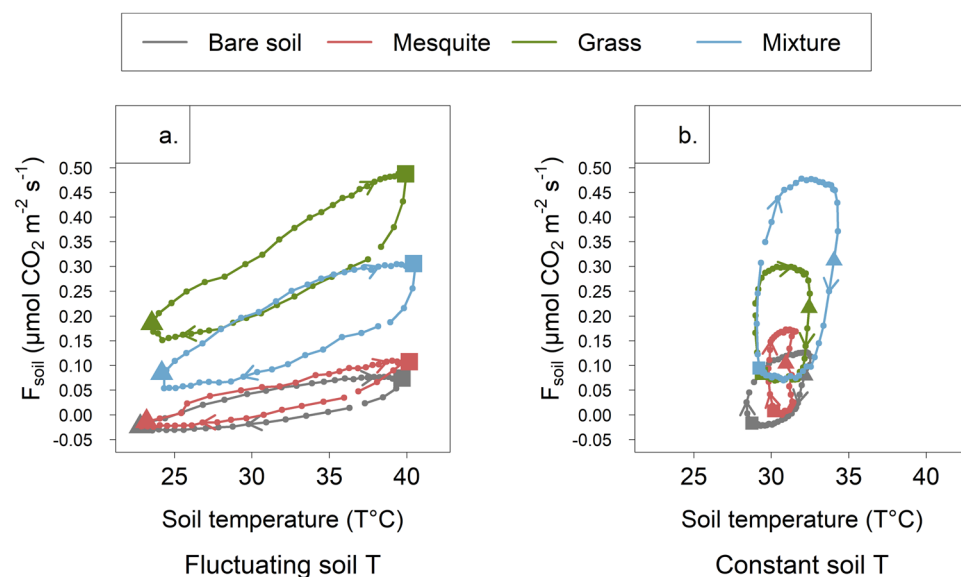


Figure 2. Average diel soil CO₂ efflux plotted against average soil temperature for all biotic treatments within soil temperature treatments. Lights were turned on at 09:30 (represented by a triangle) and shut off at 21:30 (represented by a square). Arrows represent the clockwise hysteresis detected in all situations. F_{soil} was estimated from 5 cm depth to the surface. Wet and dry conditions are computed together for each soil temperature treatment.

temperature treatment (Fig. 2). Only the amplitude of hysteresis differed, with higher values associated with mesocosms that contained grasses. Because we experimentally constrained the diel range of temperatures experienced within the “constant” treatment, the X-axis is confined to a 5 °C band, but the range of F_{soil} we detected did not change. Soil moisture did not affect general hysteric patterns (Supplementary Fig. 1). Rates of F_{soil} are very low at 20 and 50 cm depths – beyond the primary rooting depths of the plants in this experiment, underscoring a strong influence of vegetation on F_{soil} (Supplementary Fig. 2).

Differences in vegetation were the only significant driver of variation in the amplitude of the hysteric relationship between soil temperature and F_{soil} ($R^2 = 0.49$; $p < 0.001$; Fig. 3), and the presence of grasses always increased the hysteresis amplitude. We did not detect any statistical difference between the amplitudes of the hysteresis due to the imposed temperature treatment (Table 1, Fig. 3 top versus bottom panels) or targeted watering conditions (wet versus dry; Fig. 3 left versus right panels, respectively).

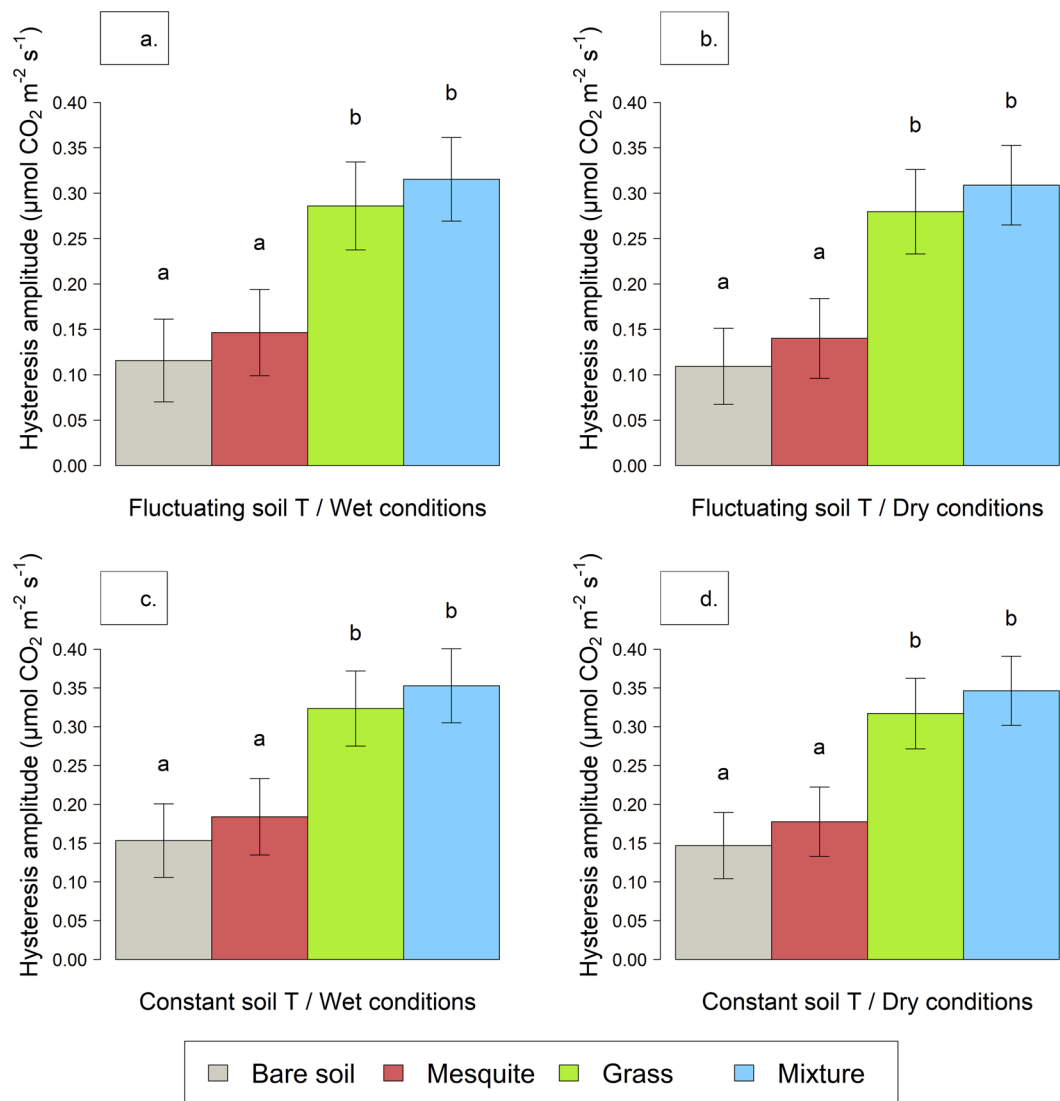


Figure 3. Adjusted mean of hysteresis amplitude (\pm standard errors) as a function of soil temperature across temperature treatments (fluctuating versus constant), targeted watering conditions (wet versus dry), and vegetation types. Letters indicate differences ($p < 0.05$) within each treatment.

Model		ANOVA degrees of freedom/ F-values/significance			
R ² m	R ² c		Soil Temperature	Soil Moisture	Vegetation type
0.40	0.49	DF (num.den)	1.44	1.44	3.44
		F-value	1.64	0.99	10.66
		p-value	0.21	0.33	<0.0001

Table 1. R², degrees of freedom, F and p-values for ANOVAs performed on the fitted model for the amplitude of hysteresis as a function of soil temperature, soil moisture and vegetation type. Non-significant interactions are not shown. R²m and R²c stand for marginal and conditional squared-R, respectively.

Average rates of net photosynthesis (A_{net}) were in most cases greater in the grasses than in the mesquites (Table 2; Fig. 4), although grasses in constant soil temperature and dry conditions did not reach higher photosynthesis levels than mesquites under the same conditions. Though both vegetative forms responded positively to wet versus dry conditions in terms of their average A_{net} , bunchgrasses were more significantly stimulated by the wet conditions.

When pooling both vegetation types, we detected a significant positive relationship between rates A_{net} and soil respiration (F_{soil} ; $R^2 = 0.29$; $p < 0.0001$) using the simple model: soil CO₂ efflux = f (photosynthesis). However, this relationship was largely driven by the high rates of A_{net} and F_{soil} within bunchgrasses ($R^2 = 0.43$; $p = 0.0046$), as there was no relationship within the mesquite mesocosms ($R^2 = 0.059$; $p = 0.3036$).

Model		ANOVA degrees of freedom/ F-values/significance							
R ² m	R ² c		S.T	S.M	SpS	S.T* S.M	S.T* SpS	S.M* SpS	S.M *S.T *SpS
0.51	0.61	DF (num.den)	1. 804	1. 804	1. 804	1. 804	1. 804	1. 804	1. 804
		F-value	171.56	27.10	197.85	45.34	135.88	15.72	6.24
		p-value	<0.0001	<0.0001	<0.0001	0.0029	<0.0001	0.0001	0.0127

Table 2. R², degrees of freedom, F statistics and p-values for ANOVAs performed on the fitted model for A_{net} as a function of soil temperature (S.T), soil moisture (S.M) and plant species grown in monoculture (SpS). R²m and R²c stand for marginal and conditional squared-R, respectively.

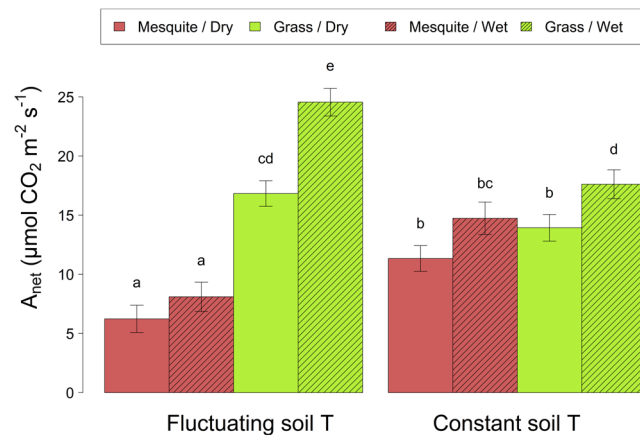


Figure 4. Adjusted mean of A_{net} (\pm standard errors) for grasses and mesquites grown in monoculture as a function of soil temperature (soil T) and moisture treatments. Lower case letters indicate differences ($p < 0.05$). Average is based on A_{net} measured from 11:30 to 19:30.

Across all vegetative types, baseline rates of F_{soil} explained the most variation in the amplitude of the hysteretic relationship between soil temperature and F_{soil} and had the most significant correlation of all potential drivers of the hysteresis (Fig. 5). Volumetric water content (VWC) explained the least amount of variation in the amplitude of the hysteretic relationship between soil temperature and F_{soil} , but we still detected a negative correlation when pooling across all vegetative cover types (Fig. 5a). However, when we examined the influence of VWC by species, we found no correlation with the amplitude of the hysteretic relationship (bare soil: $R^2 = 0.12$, $p = 0.148$; mesquite: $R^2 = 0.03$, $p = 0.5496$; grass: $R^2 = 0.03$, $p = 0.5744$; and mixture: $R^2 = 0.02$, $p = 0.6344$). Rates of A_{net} , an indirect driver of F_{soil} , had the next most significant correlation, but the effect was species specific (Fig. 5b). We found a positive correlation between the hysteresis amplitude and A_{net} within grass ($R^2 = 0.29$, $p = 0.0270$), but not within mesquite treatments ($R^2 = 0.18$, $p = 0.059$). We found that the positive correlation between the hysteresis amplitude and F_{soil} was present across all vegetative types - grass ($R^2 = 0.54$, $p = 0.0040$), mesquite ($R^2 = 0.49$, $p = 0.0081$) and mixture ($R^2 = 0.31$, $p = 0.0031$) - but not within bare soil treatments (Fig. 5c).

Discussion

Are hysteretic patterns between CO₂ efflux and soil temperature driven more by biotic or abiotic properties?

The ways in which biotic and abiotic drivers differentially determine hysteretic patterns between F_{soil} and temperature have been difficult to assess because of the potential, yet variable, roles they may play in driving rates of soil CO₂ efflux. We used controlled conditions to isolate abiotic from biotic drivers and simultaneously measured rates of aboveground photosynthetic assimilation to infer carbon source dynamics responsible for yielding different rates and temporal patterns of F_{soil} . Our results support a more biologically-driven mechanism associated with photosynthate transport in yielding the observed patterns of soil CO₂ efflux being out of sync with soil temperature. This assertion is supported by two key findings. First, we found significant and nearly equal amplitudes of clockwise hysteretic behavior between F_{soil} and soil temperature whether we allowed diel patterns of soil temperature to follow a typical sinuous curve or we held soil temperatures relatively constant. This finding is contrary to the alternative hypothesis that the hysteretic pattern stems from the differential propagation of heat through the soil profile and CO₂ diffusion because we found the same pattern behavior when there was no heat propagation through the soil. Second, we found that the amplitude of hysteresis between F_{soil} and soil temperature was most strongly tied to baseline rates of F_{soil} , which is strongly driven by the amount of fine root biomass. The majority of the residual relationship is tied to aboveground biological inputs through rates of net photosynthesis.

Others had previously hypothesized this biological driver of the hysteretic behavior based on their documentation of the phenomenon and concurrent measurements of photosynthetic rates, but no study to date had isolated photosynthetic fluxes and abiotic drivers as directly as here. For example, Vargas and Allen³¹ noted a

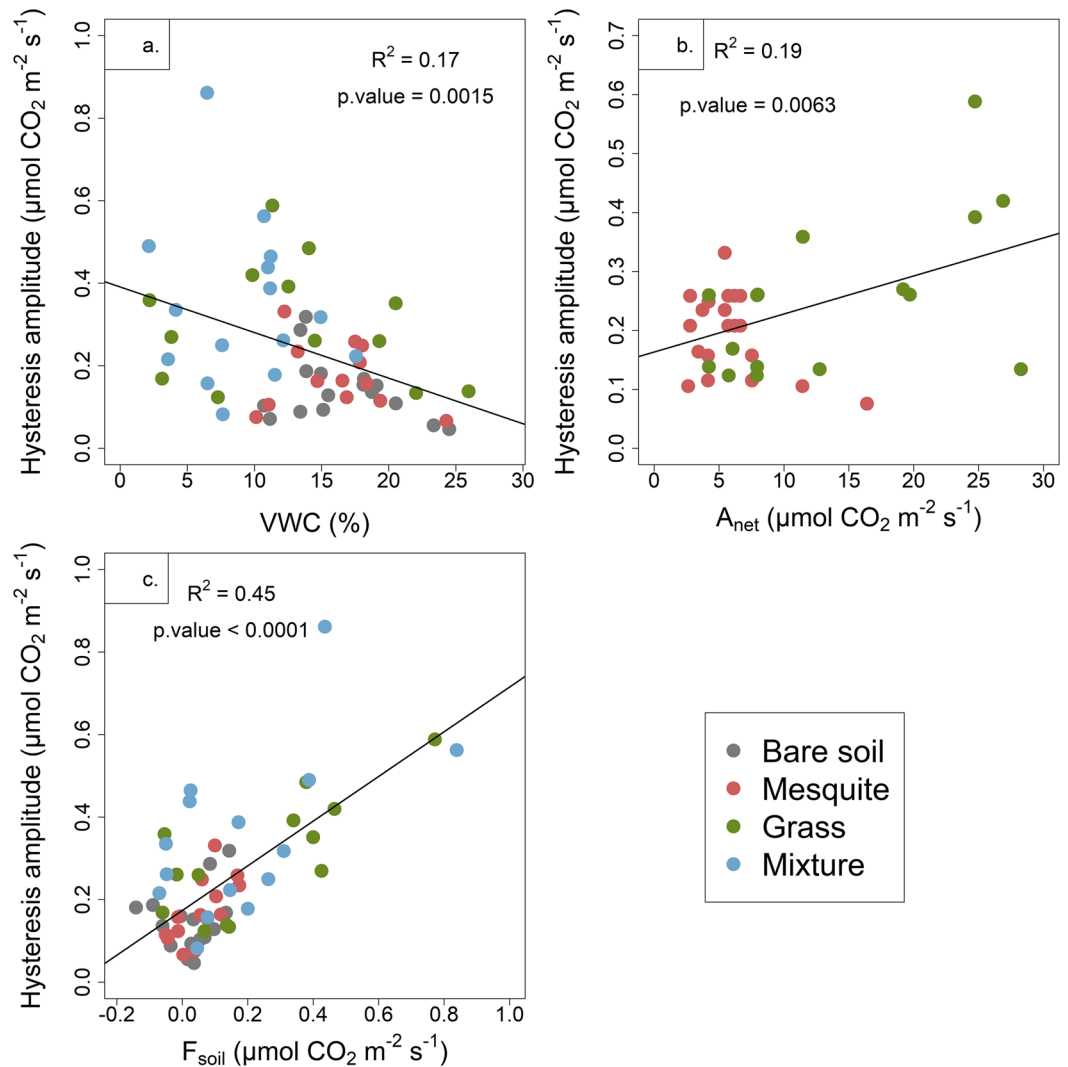


Figure 5. Illustrations of the linkages between the amplitude of hysteresis and (a) volumetric water content (VWC), (b) rates of net photosynthesis (A_{net}) in monocultures and (c) rates of F_{soil} .

relationship between F_{soil} and soil temperature that resulted in variable rates of photosynthesis in the overstory and understory vegetation under a range of natural conditions. Similarly, Barron-Gafford *et al.*⁶ found that the degree of hysteresis was positively correlated with photosynthetic rates of the overstory in a semiarid savanna. Importantly, the hysteresis observed here was greatest in mesocosms occupied by grasses. Previous research has illustrated a very short lag in the time between carbon assimilation until stimulation of F_{soil} , ranging from hours⁵⁰ to ~1 day^{14,27}. These studies, then, would suggest that same-day and day-prior photosynthesis rates were most important in determining current-day F_{soil} under bunchgrasses^{13,14,21}. Longer lag times, presumably due to longer phloem transport distance, within mesquite would reduce the correlation between these concurrent fluxes. This may explain the positive correlation we found between A_{net} and F_{soil} for bunchgrass mesocosms, but the decoupling between A_{net} and F_{soil} for mesquite mesocosms in this study.

How do contributions to the hysteretic patterns between CO₂ efflux and soil temperature vary across different plant types and environmental gradients?

Rates of net photosynthesis per unit leaf area were greater in the bunchgrasses than in the mesquite. Likewise, total leaf biomass in the bunchgrass mesocosms was six times greater than in the mesquite, and total root biomass in the bunchgrass mesocosms was nine times greater than in the mesquite. Together, these factors would yield significantly greater total photosynthate input into the soils of the mesocosm that contained bunchgrass than those that contained mesquite. This positive relationship between aboveground carbon inputs (rates of net photosynthesis) and F_{soil} is expected given that F_{soil} is the result of autotrophic and heterotrophic source of soil respiration (as recently summarized by Song *et al.*³⁶).

Differences in net photosynthetic rates in mesquite and grass tend to depend on moisture conditions, with grass having higher rates under wet conditions and mesquite having similar rates under dry and wet conditions because of the rooting strategies of mesquite that allow for greater access to deep water^{14,45,53,54}. However, these differences in net photosynthetic rates are dependent on the size and age of the woody plant, with smaller mesquites often experiencing significantly lower rates of carbon assimilation than larger individuals^{53,55–57}. Thus, the

lower photosynthetic rates in mesquite than in bunchgrass found here are in line with previous research, when considering that the mesquites were less than one year old at the time of the experiment.

The small hysteretic pattern between F_{soil} and soil temperature within the bare soil mesocosm might be surprising given that there is no vegetation to deliver photosynthetic products. However, previous research has illustrated that in dryland and Mediterranean ecosystems with alkaline soils, there can be a chemical process of carbonate precipitation and dissolution^{36,58–66}. The resulting periods of CO₂ absorption removal would contribute to a hysteretic pattern between F_{soil} and soil temperature because for the same range of temperatures one can detect daytime net CO₂ efflux, but nighttime net CO₂ influx from the atmosphere due, in part, to strong soil-air temperature gradients. The soils used here, however, contained little inorganic carbon. Even in our more strongly constrained temperature regime, some propagation of temperatures still occurred, and we suggest that it may have affected the small amount microbial activity present and likely drove some of the inorganic processes. As such, the patterns seen in the bare soil treatment likely illustrates the concomitant influence of abiotic and biotic drivers.

Conclusion

The use of precise climatic and soil condition controls allowed us to test whether the hysteretic relationship between F_{soil} and soil temperature was mainly driven by abiotic or biotic conditions. We observed a strong influence of biotic factors on hysteretic behaviors. We suggest that the delivery of photosynthate in the soil is a major factor in creating lag in the relationship between soil CO₂ efflux and soil temperature. In particular, the high photosynthetic rate and biomass of bunchgrass was associated with higher baseline rates F_{soil} and hysteresis amplitudes. Therefore, variation in plant community structure likely has an important regulatory role in governing how F_{soil} responds dynamically to climate drivers, with potentially profound impacts on seasonal ecosystem-level respiration rates.

Methods

Experimental facility and environmental monitoring. The experiment was conducted at the Ecotron Île-de-France facility (St-Pierre-les-Nemours, France), which houses a suite of highly controllable meso-scale 'Ecolabs'. Each Ecolab permits the simultaneous manipulation of multiple atmospheric parameters and climatic variables across three individual 13 m³ chamber (see Verdier *et al.*⁶⁷ for extensive technical descriptions and Supplementary Methods 1 for pictures). Within each of these chambers, there is a 1 m tall lysimeter with 1 m³ volume in which we placed four separate 60 cm tall mesocosms (0.07 m³ volume). Mesocosms were either left with bare soil or planted with the woody plant velvet mesquite (*Prosopis velutina* Woot.) only, the grass *Bouteloua curtipendula* only, or a mixed community of *P. velutina* and *B. curtipendula*. In total, six chambers and 24 mesocosm were used. We used a loamy sand-textured basalt with a porosity of 37% and bulk density of 1.5 g cm⁻³ as our soil matrix. The soil had an inorganic carbon content of 2.30×10^{-5} g g⁻¹, and a pH of 8.18; further details on the soil chemistry are previously reported^{68,69}. *P. velutina* and *B. curtipendula* seeds used in this study originated from a site located in the Santa Rita Experimental Range (31.8214°N, 110.8661°W, elevation: 1116 m) south of Tucson, Arizona, USA. This area was historically a grassland, but is now dominated by *P. velutina*, which covers approximately 35% of the ~2800 m² study site. Much of the *P. velutina* understory and intercanopy space consists of a mosaic of bunchgrasses, including *B. curtipendula*, *Eragrostis lehmanniana* Nees, *Digitaria californica* Benth, and *B. eriopoda*. Mean annual precipitation at this site is 375 mm, with about 50% falling in July-September as part of the North American Monsoon. Scott *et al.*³ described additional details on the site. We set up an establishment phase of 4 months to allow the plants to grow before the measurements. In mesocosms that include grass, 4 g of seeds were sown. As for mesquites, 30 seeds were initially sown in each mesocosm. After a month, plants were thinned to only three mesquites per mesocosm.

We monitored atmospheric CO₂ concentration ([CO₂]) using a flow-through loop linking each Ecolab chamber in-line to a gas analyzer (LI-840; LI-COR, Lincoln, Nebraska, USA). Precise control of atmospheric [CO₂] was maintained by a solenoid valves that allow for direct injection and by CO₂ absorption using soda lime when necessary. We set [CO₂] and air relative humidity at 400 ppm and 30%, respectively. Along with measures of air temperature and relative humidity, air samples were measured automatically every 30 seconds, and an average for each chamber within each Ecolab was recorded every 30 minutes. Further, we monitored soil moisture (MAS-1; Decagon Devices Inc., Pullman, WA, USA) and temperature (PT-100) at the near surface (5 cm) and at 20 cm and 50 cm depths within each replicate mesocosm. Again, measurements were conducted every 30 seconds, and we recorded an average for each mesocosm every 30 minutes. We delivered light by an overhead plasma lamp (Lumixo-A, Spectrum AM 1.5, Bulb M46, Lumartix, Aubonne, Switzerland) with a 12-hour day length that was set to occur between 09:30 and 21:30 local time.

Experimental design controlling above and belowground temperatures and soil moisture conditions.

We independently controlled above- and belowground temperatures, systematically targeting the role of abiotic versus biotic drivers of hysteretic patterns in F_{soil} . We repeated the following pair of environmental cycles under wet and dry soil moisture conditions: (i) a pattern of diel aboveground and soil temperature cycles, which mimics natural conditions of the home field site and serves as a control treatment and (ii) a pattern of diel cycle aboveground temperature but constant soil temperature. This treatment constrains vertical soil temperature gradients, a primary hypothesized abiotic driver of the hysteretic relationship between F_{soil} and soil T , while mimicking natural aboveground conditions. To reduce the amplitude of temperature variation at the surface, pipes surrounding the mesocosm surface were filled with an antifreeze liquid either to heat-up or to cool-down the system. The surface of the lysimeter was constantly maintained at 33 °C, and the bottom of the mesocosm was allowed to stabilize through heat transfer. In constant soil temperature conditions, soil cooling occurred during the daytime, whereas warming occurred during nighttime, leading to desynchronized light patterns, air temperature, and soil temperature patterns. To simulate wet conditions, mesocosms received 5 mm of tap water twice a

week using a dripping irrigation system that allowed for a slow release of water into the soil. We did not add any water during the ‘dry’ treatments to achieve dry soil moisture conditions. In order to dampen potential legacy effects of individual treatments through time experience for each of the mesocosms, we (i) randomized the timing of each treatment for each mesocosm, (ii) introduced a transition period of one week between each treatment in which the mesocosm went through the new soil moisture and soil temperature settings to allow for acclimation to the new conditions, and (iii) we ran each treatment for a two-week period. This experimental plan yielded a split-plot, repeated-measures design, allowing us to independently test for biotic versus abiotic (temperature and moisture) drivers of hysteretic behavior. The experiment lasted 7 months (4 months of establishment phase and 3 months of measurements).

Continuous estimates of soil CO₂ efflux. Building on the methods described by Barron-Gafford *et al.*⁶, we calculated F_{soil} in 30 minute increments using continuously operating solid-state CO₂ sensors (GM222, Vaisala, Helsinki, Finland). Tang *et al.*⁷⁰ provide a thorough description of the sensors operation. Briefly, each CO₂ sensor is managed by a datalogger via a multiplexer. Holes on the bottom surface of the sensor allow CO₂ to diffuse three-dimensionally through a membrane surrounding the probe. As described in detail by Pangle *et al.*⁶⁹, we extracted discrete samples of the soil gas phase through gas-sampling tubes installed in the soil at three depths of 5, 20, and 50 cm. These tubes were constructed from 0.5-m length and 0.0064-m diameter microporous Teflon tubing with pore sizes ranging from 10 to 35 μm (Parker 1 103-0125031-NT-1000, Controlled Motion Solutions). That tubing was connected to non-porous tubing, sealed together with epoxy and heat shrink tubing. Gas-phase sampling was accomplished by using a flow-through loop linked in-line to a sealed CO₂ probe housing (GMK220, Vaisala, Helsinki, Finland) with a GM222 probe inside. [CO₂] at each depth was measured for two-minute-period every 20 minutes. The probe was flushed between each measurement. [CO₂] readings were corrected for temperature and pressure using data collected by co-located sensors.

F_{soil} was calculated according to the “gradient method” using Fick’s first law of diffusion^{27,30–33,49,52,70–72}, as modified by Sanchez-Cañete *et al.*¹⁹. In previous studies^{6,39,52}, the daily degree of hysteresis was calculated as the difference between maximum and minimum F_{soil} for the daily median temperature. In our experiment, the presence of a near-constant soil temperature treatment makes the use of daily median temperatures less useful. We calculated instead a daily, microhabitat-specific amplitude of hysteresis as the difference between maximum and minimum F_{soil} for the entire day.

Leaf-level measurements of photosynthetic activity. Rates of photosynthetic CO₂ assimilation (A_{net}) were measured on twelve *P. velutina* and twelve *B. curtipendula* individuals using a portable gas-exchange system (LI-6400; LI-COR, Lincoln, Nebraska, USA), which allows the user to create a stable microenvironment inside the cuvette that mimics ambient conditions outside. Following the procedures described by Barron-Gafford *et al.*⁷³, A_{net} measurements were made continuously for a 24-hour period with the 12-hour day length. We used the LI-6400 red-blue light source (LI-6400-02b) to mimic the local levels of irradiance. Once sealed into the chamber, the leaf was acclimated to a CO₂ setpoint of 400 ppm, the ambient air temperature, the ambient relative humidity, and a constant flow rate of 700 μmol s⁻¹. Leaves placed into the cuvette were allowed to acclimate to current conditions and stabilize for a minimum of 30 minutes prior to the first gas exchange measurements. The portable photosynthesis system was then set on an auto-log procedure to match current temperature and relative humidity levels, acclimate the leaf, match the internal infrared gas analyzers, and log A_{net} upon reaching a steady value every 30 minutes. Within each species, all measures were conducted on intact leaves of similar size; we selected leaves of like age – the most recent, fully unfurled leaf. This procedure for measurements of rates of A_{net} was repeated across both temperature treatments and both wet and dry soil conditions for the three vegetated mesocosms to capture a spectrum of physiological activity, for a total of 72 individual diel measurements. Leaves were cut after each measurement to be scanned. Their area was determined using the Image J software (Schneider, Rasband & Eliceiri, 2012), allowing to calculate A_{net} per surface area.

Statistical analysis. Data analyses were performed using the R statistical software (version 3.5.1; R Core Team, 2018). Mixed effect linear models were fitted to analyse the effects of the treatments on the hysteresis amplitude and A_{net} (nlme package; Pinheiro *et al.* 2015). The data fulfilled the heteroscedasticity and normality conditions necessary to fit linear models. The experimental cells were considered as random factors in both models. The models were simplified based on the Akaike Information Criterion. For the analysis of hysteresis amplitude, the soil temperature treatments (fluctuating vs. constant), the soil moisture treatments (wet vs. dry) and the vegetation type (mesquite, grass, mixture, or bare soil) were defined as fixed factors. The model fitted for the A_{net} analysis was similar, but instead of considering 4 vegetation types, we considered only mesquite and bunchgrass. In order to focus on the general effect of plant species, only monocultures were taken into account for A_{net} . We used the A_{net} values from 11:30 to 19:30 to ensure we covered most of the daily patterns. To take into account that ecosystem functioning could change over time, the different ‘two week periods’ of measurements were included as fixed factors in models. Post-hoc pairwise comparisons were calculated from the models using the adjusted mean and Tukey-Kramer method (*lsmeans* package; Lenth 2018). The *r.squaredGLMM* function (MuMIn package; Barton 2018) was used to calculate marginal and conditional model R² such as obtaining the part of variance explained by fixed factors and random effect, respectively (Nakagawa & Schielzeth, 2013).

To analyse how the hysteresis amplitude was affected by soil water content, A_{net} and F_{soil} , person correlation analysis was used to calculate correlation coefficients. Because there is a single hysteresis amplitude value per day, we selected the value of volumetric water content, A_{net} and F_{soil} at mid-day (15:30) to test the correlation.

Received: 19 October 2018; Accepted: 26 November 2019;

Published online: 22 January 2020

References

- Schimel, D. *et al.* Contribution of increasing CO₂ and climate to carbon storage by ecosystems in the United States. *Science* **287**, 2004–2006 (2000).
- Jenerette, G. D. & Lal, R. Hydrologic sources of carbon cycling uncertainty throughout the terrestrial-aquatic continuum. *Global Change Biology* **11**, 1873–1882 (2005).
- Scott, R. L., Jenerette, G. D., Potts, D. L. & Huxman, T. E. Effects of seasonal drought on net carbon dioxide exchange from a woody-plant-encroached semiarid grassland. *Journal of Geophysical Research-Biogeosciences* **114**, 13, doi:G0400410.1029/2008jg000900 (2009).
- Barba, J. *et al.* Comparing ecosystem and soil respiration: Review and key challenges of tower-based and soil measurements. *Agricultural and Forest Meteorology* **249**, 434–443, <https://doi.org/10.1016/j.agrformet.2017.10.028> (2018).
- Law, B. E. *et al.* Spatial and temporal variation in respiration in a young ponderosa pine forests during a summer drought. *Agricultural and Forest Meteorology* **110**, 27–43 (2001).
- Barron-Gafford, G. A., Scott, R. L., Jenerette, G. D. & Huxman, T. E. The relative controls of temperature, soil moisture, and plant functional group on soil CO₂ efflux at diel, seasonal, and annual scales. *Journal of Geophysical Research - Biogeosciences* **116**, G01023, <https://doi.org/10.1029/2010JG001442> (2011).
- Baldocchi, D. D. Assessing the eddy covariance technique for evaluating carbon dioxide exchange rates of ecosystems: past, present and future. *Global Change Biology* **9**, 479–492 (2003).
- Reichstein, M. *et al.* On the separation of net ecosystem exchange into assimilation and ecosystem respiration: review and improved algorithm. *Global Change Biology* **11**, 1424–1439 (2005).
- Desai, A. R. *et al.* Cross-site evaluation of eddy covariance GPP and RE decomposition techniques. *Agricultural and Forest Meteorology* **148**, 821–838, <https://doi.org/10.1016/j.agrformet.2007.11.012> (2008).
- Mahecha, M. D. *et al.* Global convergence in the temperature sensitivity of respiration at ecosystem level. *Science* **329**, 838–840, <https://doi.org/10.1126/science.1189587> (2010).
- Savage, K., Davidson, E. A. & Tang, J. Diel patterns of autotrophic and heterotrophic respiration among phenological stages. *Global Change Biology* <https://doi.org/10.1111/gcb.12108> (2012).
- Vargas, R. *et al.* On the multi-temporal correlation between photosynthesis and soil CO₂ efflux: reconciling lags and observations. *New Phytologist* **191**: no. <https://doi.org/10.1111/j.1469-8137.2011.03771.x> (2011).
- Ogle, K. *et al.* Quantifying ecological memory in plant and ecosystem processes. *Ecology Letters* **18**, 221–235, <https://doi.org/10.1111/ele.12399> (2015).
- Barron-Gafford, G. A. *et al.* Quantifying the timescales over which exogenous and endogenous conditions affect soil respiration. *New Phytologist* **202**, 442–454, <https://doi.org/10.1111/nph.12675> (2014).
- Lloyd, J. & Taylor, J. A. On the temperature-dependence of soil respiration. *Functional Ecology* **8**, 315–323 (1994).
- Cable, J. M., Ogle, K., Tyler, A. P., Pavao-Zuckerman, M. A. & Huxman, T. E. Woody plant encroachment impacts on soil carbon and microbial processes: results from a hierarchical Bayesian analysis of soil incubation data. *Plant and Soil* **320**, 153–167, <https://doi.org/10.1007/s11104-008-9880-1> (2009).
- Jin, Z., Dong, Y. S., Qi, Y. C. & An, Z. S. Soil respiration and net primary productivity in perennial grass and desert shrub ecosystems at the Ordos Plateau of Inner Mongolia, China. *Journal of Arid Environments* **74**, 1248–1256, <https://doi.org/10.1016/j.jaridenv.2010.05.018> (2010).
- Zhang, N., Zhao, Y.-S. & Yu, G.-R. Simulated annual carbon fluxes of grassland ecosystems in extremely arid conditions. *Ecological Research* **24**, 185–206, <https://doi.org/10.1007/s11284-008-0497-x> (2009).
- Sanchez-Canete, E. P., Scott, R. L., van Haren, J. & Barron-Gafford, G. A. Improving the accuracy of the gradient method for determining soil carbon dioxide efflux. *Journal of Geophysical Research-Biogeosciences* **122**, 50–64, <https://doi.org/10.1002/2016jg003530> (2017).
- Zhou, X. H. *et al.* Concurrent and lagged impacts of an anomalously warm year on autotrophic and heterotrophic components of soil respiration: a deconvolution analysis. *New Phytologist* **187**, 184–198, <https://doi.org/10.1111/j.1469-8137.2010.03256.x> (2011).
- Cable, J. M. *et al.* Antecedent conditions influence soil respiration differences in shrub and grass patches. *Ecosystems* **16**, 1230–1247, <https://doi.org/10.1007/s10021-013-9679-7> (2013).
- Cueva, A., Bahn, M., Litvak, M., Pumpanen, J. & Vargas, R. A multisite analysis of temporal random errors in soil CO₂ efflux. *Journal of Geophysical Research-Biogeosciences* **120**, 737–751, <https://doi.org/10.1002/2014jg002690> (2015).
- Davidson, E. A., Samanta, S., Caramori, S. S. & Savage, K. The Dual Arrhenius and Michaelis-Menten kinetics model for decomposition of soil organic matter at hourly to seasonal time scales. *Global Change Biology* **18**, 371–384, <https://doi.org/10.1111/j.1365-2486.2011.02546.x> (2012).
- Ogle, K., Ryan, E., Dijkstra, F. A. & Pendall, E. Quantifying and reducing uncertainties in estimated soil CO₂ fluxes with hierarchical data-model integration. *Journal of Geophysical Research-Biogeosciences* **121**, 2935–2948, <https://doi.org/10.1002/2016jg003385> (2016).
- Raich, J. W. & Schlesinger, W. H. The global carbon-dioxide flux in soil respiration and its relationship to vegetation and climate. *Tellus Series B-Chemical and Physical Meteorology* **44**, 81–99 (1992).
- Parkin, T. B. & Kaspar, T. C. Temperature controls on diurnal carbon dioxide flux: Implications for estimating soil carbon loss. *Soil Science Society of America Journal* **67**, 1763–1772 (2003).
- Tang, J. W., Baldocchi, D. D. & Xu, L. Tree photosynthesis modulates soil respiration on a diurnal time scale. *Global Change Biology* **11**, 1298–1304 (2005).
- Gaumont-Guay, D. *et al.* Interpreting the dependence of soil respiration on soil temperature and water content in a boreal aspen stand. *Agricultural And Forest Meteorology* **140**, 220–235 (2006).
- Carbone, M. S., Winston, G. C. & Trumbore, S. E. Soil respiration in perennial grass and shrub ecosystems: Linking environmental controls with plant and microbial sources on seasonal and diel timescales. *Journal of Geophysical Research-Biogeosciences* **113** (2008).
- Riveros-Iregui, D. A., McGlynn, B. L., Epstein, H. E. & Welsch, D. L. Interpretation and evaluation of combined measurement techniques for soil CO₂ efflux: Discrete surface chambers and continuous soil CO₂ concentration probes. *Journal of Geophysical Research-Biogeosciences* **113** (2008).
- Vargas, R. & Allen, M. F. Diel patterns of soil respiration in a tropical forest after Hurricane Wilma. *Journal of Geophysical Research-Biogeosciences* **113** (2008a).
- Vargas, R. & Allen, M. F. Dynamics of fine root, fungal rhizomorphs, and soil respiration in a mixed temperate forest: Integrating sensors and observations. *Vadose Zone Journal* **7**, 1055–1064 (2008b).
- Vargas, R. & Allen, M. F. Environmental controls and the influence of vegetation type, fine roots and rhizomorphs on diel and seasonal variation in soil respiration. *New Phytologist* **179**, 460–471 (2008).
- Liu, Z., Zhang, Y. Q., Fa, K. Y., Qin, S. G. & She, W. W. Rainfall pulses modify soil carbon emission in a semiarid desert. *Catena* **155**, 147–155, <https://doi.org/10.1016/j.catena.2017.03.011> (2017).
- Zhong, Y. Q. W., Yan, W. M., Zong, Y. Z. & Shanguan, Z. P. Biotic and abiotic controls on the diel and seasonal variation in soil respiration and its components in a wheat field under long-term nitrogen fertilization. *Field Crop. Res.* **199**, 1–9, <https://doi.org/10.1016/j.fcr.2016.09.014> (2016).
- Song, W. M. *et al.* Contrasting diel hysteresis between soil autotrophic and heterotrophic respiration in a desert ecosystem under different rainfall scenarios. *Scientific Reports* **5**, <https://doi.org/10.1038/srep16779> (2015).

37. Zhang, Q. *et al.* The hysteresis response of soil CO₂ concentration and soil respiration to soil temperature. *Journal of Geophysical Research-Biogeosciences* **120**, 1605–1618, <https://doi.org/10.1002/2015jg003047> (2015).
38. Liu, J. B. *et al.* Abiotic CO₂ exchange between soil and atmosphere and its response to temperature. *Environmental Earth Sciences* **73**, 2463–2471, <https://doi.org/10.1007/s12665-014-3595-9> (2015).
39. Oikawa, P. Y. *et al.* Unifying soil respiration pulses, inhibition, and temperature hysteresis through dynamics of labile soil carbon and O₂. *Journal of Geophysical Research-Biogeosciences* **119**, 521–536, <https://doi.org/10.1002/2013jg002434> (2014).
40. Wang, B. *et al.* Soil water regulates the control of photosynthesis on diel hysteresis between soil respiration and temperature in a desert shrubland. *Biogeosciences* **14**, 3899–3908, <https://doi.org/10.5194/bg-14-3899-2017> (2017).
41. Wang, B. *et al.* Soil moisture modifies the response of soil respiration to temperature in a desert shrub ecosystem. *Biogeosciences* **11**, 259–268, <https://doi.org/10.5194/bg-11-259-2014> (2014).
42. Hamilton, E. W., Heckathorn, S. A., Joshi, P., Wang, D. & Barua, D. Interactive effects of elevated CO₂ and growth temperature on the tolerance of photosynthesis to acute heat stress in C3 and C4 Species. *Journal of Integrative Plant Biology* **50**, 1375–1387, <https://doi.org/10.1111/j.1744-7909.2008.00747.x> (2008).
43. Potts, D. L., Barron-Gafford, G. A. & Jenerette, G. D. Metabolic acceleration quantifies biological systems' ability to up-regulate metabolism in response to episodic resource availability. *Journal of Arid Environments* **104**, 9–16, <https://doi.org/10.1016/j.jaridenv.2014.01.018> (2014).
44. Potts, D. L. *et al.* Antecedent moisture and seasonal precipitation influence the response of canopy-scale carbon and water exchange to rainfall pulses in a semi-arid grassland. *New Phytologist* **170**, 849–860 (2006).
45. Barron-Gafford, G. A. *et al.* Impacts of hydraulic redistribution on grass-tree competition vs facilitation in a semi-arid savanna. *New Phytologist* **215**, 1451–1461, <https://doi.org/10.1111/nph.14693> (2017).
46. Ekblad, A. & Hogberg, P. Natural abundance of ¹³C in CO₂ respired from forest soils reveals speed of link between tree photosynthesis and root respiration. *Oecologia* **127**, 305–308 (2001).
47. Högberg, P. *et al.* Large-scale forest girdling shows that current photosynthesis drives soil respiration. *Nature* **411**, 789–792 (2001).
48. Thompson, M. V. & Holbrook, N. M. Application of a singlesolute non-steady-state phloem model to the study of long-distance assimilate transport. *Journal of Theoretical Biology* **220**, 419–455 (2003).
49. Baldocchi, D., Tang, J. & Xu, L. How switches and lags in biophysical regulators affect spatial-temporal variation of soil respiration in an oak-grass savanna. *Journal of Geophysical Research* **111**, G02008, doi:02010.01029/02005JG000063. (2006).
50. Carbone, M. S. & Trumbore, S. E. Contribution of new photosynthetic assimilates to respiration by perennial grasses and shrubs: residence times and allocation patterns. *New Phytologist* **176**, 124–135 (2007).
51. Phillips, C. L., Nickerson, N., Risk, D. & Bond, B. J. Interpreting diel hysteresis between soil respiration and temperature. *Global Change Biology* <https://doi.org/10.1111/j.1365-2486.2010.02250>. (2010).
52. Riveros-Iregui, D. A. *et al.* Diurnal hysteresis between soil CO₂ and soil temperature is controlled by soil water content. *Geophysical Research Letters* **34** (2007).
53. Barron-Gafford, G. A., Scott, R. L., Jenerette, G. D., Hamerlynck, E. P. & Huxman, T. E. Temperature and precipitation controls over leaf- and ecosystem-level CO₂ flux along a woody plant encroachment gradient. *Global Change Biology* **18**, 1389–1400, <https://doi.org/10.1111/j.1365-2486.2011.02599.x> (2012).
54. Barron-Gafford, G. A., Scott, R. L., Jenerette, G. D., Hamerlynck, E. P. & Huxman, T. E. Landscape and environmental controls over leaf and ecosystem carbon dioxide fluxes under woody plant expansion. *J. Ecol.* **101**, 1471–1483, <https://doi.org/10.1111/1365-2745.12161> (2013).
55. Potts, D. L., Scott, R. L., Cable, J. M., Huxman, T. E. & Williams, D. G. Sensitivity of mesquite shrubland CO₂ exchange to precipitation in contrasting landscape settings. *Ecology* **89**, 2900–2910 (2008).
56. Potts, D. L., Huxman, T. E., Scott, R. L., Williams, D. G. & Goodrich, D. C. The sensitivity of ecosystem carbon exchange to seasonal precipitation and woody plant encroachment. *Oecologia* **150**, 453–463 (2006).
57. De Soyza, A. G., Franc, A. C., Virginia, R. A., Reynolds, J. E. & Whitford, W. G. Effects of plant size on photosynthesis and water relations in the desert shrub *Prosopis glandulosa* (Fabaceae). *American Journal of Botany* **83**, 99–105 (1996).
58. Hamerlynck, E. P., Scott, R. L., Sanchez-Cañete, E. P. & Barron-Gafford, G. A. Nocturnal soil CO₂ uptake and its relationship to subsurface soil and ecosystem carbon fluxes in a Chihuahuan Desert shrubland. *Journal of Geophysical Research-Biogeosciences* **118**, 1593–1603, <https://doi.org/10.1002/2013jg002495> (2013).
59. Angert, A. *et al.* Using O₂ to study the relationships between soil CO₂ efflux and soil respiration. *Biogeosciences* **12**, 2089–2099, <https://doi.org/10.5194/bg-12-2089-2015> (2015).
60. Ma, J., Liu, R. & Li, Y. Abiotic contribution to total soil CO₂ flux across a broad range of land-cover types in a desert region. *Journal of Arid Land* **9**, 13–26, <https://doi.org/10.1007/s40333-016-0061-4> (2017).
61. Emmerich, W. E. Carbon dioxide fluxes in a semiarid environment with high carbonate soils. *Agricultural and Forest Meteorology* **116**, 91–102, [https://doi.org/10.1016/s0168-1923\(02\)00231-9](https://doi.org/10.1016/s0168-1923(02)00231-9) (2003).
62. Sánchez-Cañete, E. P., Chorover, J. & Barron-Gafford, G. A. A considerable fraction of soil-respired CO₂ is not emitted directly to the atmosphere. *Nature Scientific Reports* (2018).
63. Mielnick, P., Dugas, W. A., Mitchell, K. & Havstad, K. Long-term measurements of CO₂ flux and evapotranspiration in a Chihuahuan desert grassland. *Journal of Arid Environments* **60**, 423–436, <https://doi.org/10.1016/j.jaridenv.2004.06.001> (2005).
64. Stevenson, B. A. & Verburg, P. S. J. Effluxed CO₂-C¹³ from sterilized and unsterilized treatments of a calcareous soil. *Soil Biology & Biochemistry* **38**, 1727–1733, <https://doi.org/10.1016/j.soilbio.2005.11.028> (2006).
65. Stone, R. Ecosystems - Have desert researchers discovered a hidden loop in the carbon cycle? *Science* **320**, 1409–1410, <https://doi.org/10.1126/science.320.5882.1409> (2008).
66. Sanchez-Cañete, E. P., Kowalski, A. S., Serrano-Ortiz, P., Perez-Priego, O. & Domingo, F. Deep CO₂ soil inhalation/exhalation induced by synoptic pressure changes and atmospheric tides in a carbonated semiarid steppe. *Biogeosciences* **10**, 6591–6600, <https://doi.org/10.5194/bg-10-6591-2013> (2013).
67. Verdier, B. *et al.* Climate and atmosphere simulator for experiments on ecological systems in changing environments. *Environmental Science & Technology* **48**, 8744–8753, <https://doi.org/10.1021/es405467s> (2014).
68. van Haren, J. *et al.* CO₂ diffusion into pore spaces limits weathering rate of an experimental basalt landscape. *Geology* **45**, 203–206, <https://doi.org/10.1130/g38569.1> (2017).
69. Pangle, L. A. *et al.* The Landscape Evolution Observatory: A large-scale controllable infrastructure to study coupled Earth-surface processes. *Geomorphology* **244**, 190–203, <https://doi.org/10.1016/j.geomorph.2015.01.020> (2015).
70. Tang, J. W., Baldocchi, D. D., Qi, Y. & Xu, L. K. Assessing soil CO₂ efflux using continuous measurements of CO₂ profiles in soils with small solid-state sensors. *Agricultural and Forest Meteorology* **118**, 207–220 (2003).
71. Tang, J. W., Misson, L., Gershenson, A., Cheng, W. X. & Goldstein, A. H. Continuous measurements of soil respiration with and without roots in a ponderosa pine plantation in the Sierra Nevada Mountains. *Agricultural and Forest Meteorology* **132**, 212–227 (2005).
72. Myklebust, M. C., Hipps, L. E. & Ryel, R. J. Comparison of eddy covariance, chamber, and gradient methods of measuring soil CO₂ efflux in an annual semi-arid grass, *Bromus tectorum*. *Agricultural and Forest Meteorology* **148**, 1894–1907 (2008).
73. Barron-Gafford, G. A. *et al.* Herbivory of wild *Manduca sexta* causes fast down-regulation of photosynthetic efficiency in *Datura wrightii*: an early signaling cascade visualized by chlorophyll fluorescence. *Photosynthesis Research* **113**, 249–260, <https://doi.org/10.1007/s11220-012-9741-x> (2012).

Acknowledgements

The experiment, data acquisition, and collaborations were supported by funding to R. Ferrière under the program “Investissements d’Avenir” launched by the French government and implemented by ANR with the reference ANR-10-IDEX-0001-02 PSL (EXPECTS project), under the CNRS Eco-Evo-Devo Pépinière program and under the Partner University Funds program 2013 between ENS and University of Arizona (UofA). Additional funding in United States was provided by the Philecology Foundation (Fort Worth, Texas, USA) and its founder, Mr. Edward Bass, and the Thomas R. Brown Family Foundation. This work has benefited from technical and human resources provided by the CNRS IR ECOTRONS and CEREEP-Ecotron IleDeFrance (CNRS/ENS UMS 3194) as well as financial support from the Regional Council of Ile-de-France under the DIM Program R2DS bearing the references I-05-098/R and 2011-11017735 and from the European Union FEDER program 2007–2013. It has received a support under the program “Investissements d’Avenir” launched by the French government and implemented by ANR with the reference ANR-11-INBS-0001 AnaEE France. This project and data were also supported by NSF awards 1417101 and 1331408 to G. Barron-Gafford, as well as by a Marie Curie International Outgoing Fellowship within the Seventh European Community Framework Programme, DIESEL project (625988) to E.P. Sanchez-Cañete. Additional awards provided travel support to G. Barron-Gafford from the UofA Office of Global Initiatives, the Office of the Vice President of Research at the UofA, and the UMI iGLOBES program at the UofA. The authors thank Ken Coppola at the Desert Legume Program (DELEP) in Tucson, Arizona, who provided seeds for the experiment from the field site.

Author contributions

Y.D., S.C., F.M., M.L., A.H., and S.J. established research sites and installed monitoring equipment. G.A.B.-G., E.P.S.-C., J.F.L.G., K.D., J.v.H., M.A.P.-Z. designed the experiment, and Y.D. directed the research and conducted the statistics. S.C. directed data acquisition and processing. J.F.L.G., R.F., E.P.S.-C., and P.T. led efforts to secure funding for the research. Y.D., E.P.H., and G.A.B.-G. led the manuscript preparation, and all authors discussed the results and contributed to the manuscript.

Competing interests

The authors declare no competing interests.

Additional information

Supplementary information is available for this paper at <https://doi.org/10.1038/s41598-019-55390-6>.

Correspondence and requests for materials should be addressed to Y.D.

Reprints and permissions information is available at www.nature.com/reprints.

Publisher’s note Springer Nature remains neutral with regard to jurisdictional claims in published maps and institutional affiliations.



Open Access This article is licensed under a Creative Commons Attribution 4.0 International License, which permits use, sharing, adaptation, distribution and reproduction in any medium or format, as long as you give appropriate credit to the original author(s) and the source, provide a link to the Creative Commons license, and indicate if changes were made. The images or other third party material in this article are included in the article’s Creative Commons license, unless indicated otherwise in a credit line to the material. If material is not included in the article’s Creative Commons license and your intended use is not permitted by statutory regulation or exceeds the permitted use, you will need to obtain permission directly from the copyright holder. To view a copy of this license, visit <http://creativecommons.org/licenses/by/4.0/>.

© The Author(s) 2020